Global Optimization of High Harmonic Generation

S. Kazamias, D. Douillet, F. Weihe, C. Valentin, A. Rousse, S. Sebban, G. Grillon, F. Augé, D. Hulin, and Ph. Balcou

Laboratoire d'Optique Appliquée, ENSTA- Ecole Polytechnique, CNRS UMR 7639, F-91761 Palaiseau CEDEX, France

(Received 9 October 2002; published 15 May 2003)

We investigate the relevance of the absorption limit concept in the optimization of high harmonic generation. Thanks to the first direct observation of the coherence length of the process from high-contrast Maker fringes, we unravel experimental conditions for which the harmonic dipole response is enhanced when phase matching is realized within the absorption limit, leading to record conversion efficiencies in argon. Moreover, we show that harmonic generation in guided or freely propagating geometries are equivalent in the loose focusing regime. This analysis is generalized to other advanced phase-matching schemes, thereby predicting the possibility to boost the conversion efficiencies using light noble gases.

DOI: 10.1103/PhysRevLett.90.193901 PACS numbers: 42.65.Ky, 32.80.Rm

Among the various techniques considered to obtain femtosecond extreme ultraviolet (XUV) light sources, laser-based high-order harmonics generated in noble gases now have a prominent position, thanks to the compactness of the setup, and their unique capability to reach attosecond resolution [1,2]. Those features can complement larger installations, such as x-ray free-electron lasers currently under development. From an application standpoint, the choice between these very different types of sources mostly comes from any of two factors, the repetition rate of the source, and the brightness, related to the conversion efficiency from laser to XUV light. Efficiency optimization for high harmonics was recently thought to be achieved, as several groups reported phase-matched generation [3], and then reached the so-called "absorption limit," for which reabsorption limits the effective medium length [4,5].

Surprisingly, it turns out, however, that published conversion efficiencies still depend widely on the generation geometry, even within this absorption limit. In particular, high-energy lasers were used recently to enhance harmonic fluxes [6,7], and we show here that very high efficiencies can also be obtained using an argon gas cell subjected to a freely propagating, very loosely focused 2 mJ laser. Such a wide span of results demonstrates that ultimate optimization conditions are far from being fully characterized.

The aim of the present Letter is to show how different macroscopic results may be obtained from high harmonic generation, even in absorption-limited conditions. From a one-dimensional model, we determine the loose focusing condition for which harmonics created by a freely propagating beam in a gas cell benefit from the same homogeneous phase matching as in hollow-core fibers [3]. We then explore how the interplay between single atom response, and macroscopic phase matching can be tailored to enhance the efficiencies, as demonstrated experimentally. We eventually investigate how advanced phase-matching schemes may further optimize the yields.

In the current understanding, perfect phase matching of high harmonics is transiently realized when the positive atomic gas dispersion is balanced by the negative dispersion factors, i.e., the modal dispersion in fibers [3], or the free-electron dispersion [8]. The experimental phase matching between harmonic dipoles within the medium is characterized by the coherence length l_{coh}, over which the harmonic field can build up constructively. Amazingly, no actual measurements of coherence lengths based on interference Maker fringes [9] were presented since the first evidence in 1992 [10]. We report the first experimental demonstration of high-contrast fringes in high harmonic generation (HHG), making possible the concrete understanding of phase-matching optimization.

We use a 35 fs, 1 kHz Ti:sapphire laser system, centered at $\lambda = 805$ nm; 2 mJ laser pulses are loosely focused into the medium ($f/100$ focusing) [11], resulting in a Rayleigh length $z_0 = 17$ mm. The gas target consists of an adjustable length gas cell in vacuum. The pressure in it can also be easily varied. High harmonics produced on axis are first separated from the infrared by aluminum filters, then analyzed by a transmission-grating spectrometer, coupled to a back-illuminated XUV charge-coupled device (CCD) camera. The spectrometer collection angle is 2 mrad, so that only highly collimated light is detected. All spectrometer elements are calibrated, allowing us to infer absolute harmonic yields.

Figure 1(a) shows how the signal from harmonic 23 in argon varies with the cell length. The cell entrance position z_C is located 2 mm before, after, or on the beam focus ($z_C > 0$ means the cell is after the focus). At $z_C = -2$ mm, high-contrast Maker fringes can be observed, with a coherence length of 0.75 mm. Strikingly, the Maker fringes vanish when the focus is displaced beyond the cell entrance: The signal keeps growing with a quadratic rise, typical of phase matching.

Based on these results, we searched for conditions optimizing high harmonic fluxes, using long gas cells. Positioning the cell up to 16 mm after the focus resulted

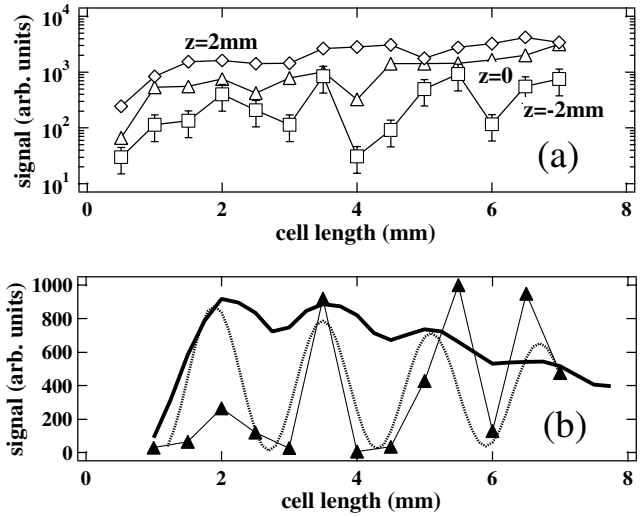

FIG. 1. (a) Maker fringes observed on gas cell length dependences of harmonic 23, when the cell entrance is located before the focus ($z_C = -2$ mm, squares), at focus ($z_C = 0$ mm, triangles), or after it ($z_C = 2$ mm, diamonds). (b) Comparison between the experimental Maker fringes of harmonic 25 ($z_C = -2$ mm, triangles), with the time-independent phase-matching fit (3) (dashed line), and the time-dependent 1D code (solid line).

in enhanced yields of harmonics 21 to 27. The conversion efficiency then reaches $1.5(\pm 0.5) \times 10^{-5}$ for harmonic 21, and up to $3(\pm 1) \times 10^{-5}$ for harmonic 23, which is the highest reported thus far in argon, to the best of our knowledge.

Such asymmetrical yields, with respect to the medium position relative to focus, are known to be due to the role of the dipole phase gradient, due to intensity gradient [12,13]. Our results demonstrate therefore that the dipole phase does play an important role to boost the yields, whereas such effects were thus far neglected in reports of absorption-limited yields [5].

These experimental findings can be understood in the framework of a one-dimensional model that generalizes the model proposed by Durfee *et al.* [14] or Constant *et al.* [4], and is able to fully describe on-axis phase matching for an arbitrary laser beam, describing either a guided-wave geometry, or free space focusing.

The laser electric field $E(z, \tau)$, where τ is the time in the moving frame of the pulse, induces dipole moments $d_q(z, \tau)$ at the qth harmonic frequency $q\omega$, where ω is the laser angular frequency. This harmonic response arises from two main quantum paths, corresponding to electron trajectories that have spent different times in the continuum, leading to different quantum phases [15]. Following Ref. [15], we disentangle the contribution of each quantum path l from the total dipole moment, as $d_q^l = \chi_l |E|^\nu \exp(-i\alpha_l I)$, where I is the laser intensity. The amplitude exponent ν [16] characterizes the intensity behavior, and depends mostly on the nature of the gas target. The phase coefficient α is usually negligible for the first path ($\alpha_1 \approx 10^{-14}$ cm^2/W), but quite large for the second one ($\alpha_2 \approx 25 \times 10^{-14}$ cm^2/W).

The microscopic response of the medium is obtained via the full dipole calculation given by the theory of Lewenstein [15], modified to take into account the well-accepted Ammosov-Delone-Krainov ionization rates. The propagation calculation is then performed separately for each path component l, so that the time-dependent harmonic field at the exit of the medium reads

$$E_q(L, \tau) = \frac{iq\omega}{\epsilon_0 c} \sum_l \int_{z_C}^{z_C+L} dz N_0 \chi_l |E|^\nu e^{i\Phi(z,\tau)+(z-L)/(2L_{\text{abs}})}. \tag{1}$$

Here, N_0 is the space- and time-dependent atomic density, L_{abs} is the absorption length, and the total propagation phase is $\Phi(z, \tau) = q\Phi_1(z_C, z) + \Phi_q(z, z_C + L) - \alpha_l I(z)$, where $\Phi_1(z_C, z)$ and $\Phi_q(z, z_C + L)$ are, respectively, the propagation phases of the infrared from the medium entrance to z, and of the high harmonic from z to the medium exit.

Phase matching can be evaluated by expanding the total phase as $\Phi(z, \tau) = \Phi(L, \tau) + \delta k(\tau)(z - L) + \delta k^{(2)}(\tau)(z - L)^2$. The first-order term corresponds to the usual time-dependent wave-vector mismatch $\delta k = \pi / L_{\text{coh}}$, whereas the second describes the inhomogeneity of phase-matching conditions. Efficient harmonic generation implies (i) that there is a large time interval within the pulse when $\delta k(\tau)$ vanishes to within $1/5 L_{\text{abs}}$ [4] and (ii) that during this time the second-order term evaluated over the cell length remains much smaller than $\pi/2$.

To illustrate this requirement, Fig. 2 displays $\Phi(z)$ for harmonic 23 in argon in a 3-mm-long cell, for three Gaussian focusing conditions, from rather strong to intermediate and very loose focusing ($z_0 = 3$, 10, and 30 mm, respectively), at a time when phase matching is realized at the cell output (laser focus is at the entrance). For $z_0 = 3$ mm, the initial part of the medium is simply not phase matched, when phase matching is realized at the exit. It takes a very loose focusing geometry for the phase to remain basically constant (i.e., $z_0 = 30$ mm).

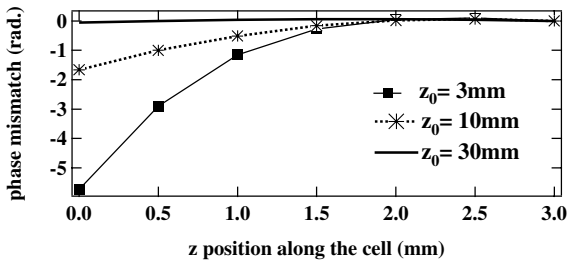

FIG. 2. Total phase $\Phi(z)$ of H23 in a 15 Torr Ar medium, when phase matching is realized at the output of the medium, for Gaussian beams of Rayleigh ranges of 3, 10, and 30 mm (respectively solid, dashed, and dotted line).

Studying the dispersion terms allows us to estimate this curvature effect of $\Phi(z)$. Taking the ionization probability to vary as I^{ν}, and evaluating the wave-vector mismatch at the input of a $3L_{\mathrm{abs}}$-long medium when the output is phase matched, results in the following empirical criterion:

$$z_0 > \sqrt{\frac{45}{\pi} L_{\mathrm{abs}}^3 \frac{q\omega}{c} \nu P_{\mathrm{ion}}(\delta k = 0)\left(\frac{N_0}{2n_c} + \delta n_{\mathrm{at}}\right)}, \qquad (2)$$

where $P_{\mathrm{ion}}(\delta k = 0)$ is the ionization probability at the time of phase matching at the cell exit, and n_c the electron critical density. In this regime, the linear phase approximation of Ref. [4] is therefore valid, and one recovers completely the physics of guided-wave propagation discussed in Ref. [14]. This reconciles therefore the physics of HHG in hollow-core fibers [3,14], and those of HHG in gas cells or jets in the very loose focusing limit. Our experimental data were taken in conditions close to satisfy (2); in that case, l_{coh} is constant over the medium and the instantaneous harmonic flux emitted on axis is proportional to the product of the dipole amplitude by a phase-matching factor between 0 and 1, equal to 1 in absorption-limited conditions:

$$F_q = \frac{1}{1 + \frac{4\pi^2 L_{\mathrm{abs}}^2}{L_{\mathrm{coh}}^2}}\left[1 + e^{-L/L_{\mathrm{abs}}} - 2\cos\frac{\pi L}{L_{\mathrm{coh}}} e^{-[L/(2L_{\mathrm{abs}})]}\right]. \qquad (3)$$

The solid line in Fig. 1(b) shows the result of the full integration of (1) to model the Maker fringes, compared to a simple fit based on Eq. (3) (dashed line). Even though the model does not include any adjustable parameter, it reproduces and explains the observed fringe period which corresponds to twice the coherence length at the time when the harmonic reaches the plateau.

This agreement between experimental phase-matching features and our 1D model enables us to explore the temporal interplay between the phase-matching mechanism and dipole response. The first-order time-dependent wave-vector mismatch leading to F_q is $\delta k(\tau) = (q\omega/c)(\delta n_{\mathrm{at}} + \delta n_{\mathrm{el}}) + q\partial_z \Phi_{\mathrm{geom}} + \partial_z \Psi_l$, where Φ_{geom} is the geometrical phase slip incurred by the laser beam, corresponding either to the focusing Gouy phase or to the phase drift for a guided wave, δn_{at} and δn_{el} represent the deviations from 1 of the refractive index, due to the positive atomic and negative electronic dispersion, and Ψ_l denotes the atomic dipole phase.

Figure 3 displays the time-dependent phase-matching factor [Eq. (3)] and dipole for typical cases. Figure 3(a) presents the phase-matching case based on a balance between atomic and geometrical dispersion obtained in capillary waveguides, computed for the low-intensity regime of Ref. [14]: The phase-matching factor is very high throughout the pulse, but the dipole remains low.

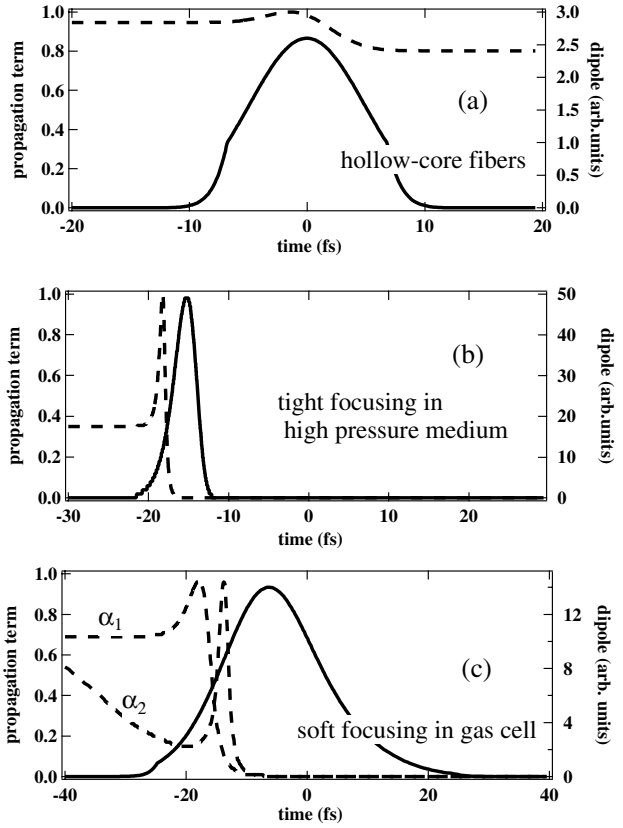

FIG. 3. Time dependence of the amplitude phase-matching factor (3) and harmonic dipole (a) in a hollow-core fiber geometry, (b) in a short cell/high density configuration, and (c) in our experimental conditions for $z_c = 16$ mm, considering the first (dashed line), and second (solid line) quantum paths. Time is scaled with the pulses HWHM.

Figure 3(b) presents the opposite limit in the high-density high-intensity conditions of Ref. [5]. As compared to the previous case, the phase-matching factor is close to 1 during a much shorter time but the dipole moments reach much higher values: The global conversion efficiency is thus increased.

In our experimental conditions, the dipole phase can no longer be neglected. Figure 3(c) displays the phase-matching factor calculated for the two main quantum paths. The phase-matching spike is still clearly visible. Interestingly, the phase gradient due to the second path [15] allows phase matching to be realized on axis at higher ionization rates, at a time when the atomic response is higher. The enhancement between $z_C = -2$ and 2 mm (Fig. 1) can be explained by the opposite signs of the phase gradients: If condition (2) is fulfilled, phase matching is realized when the cell is placed after the focus, in contrast to the previous strong focusing regime [12]. Therefore, the absorption limit should not be considered as an absolute limit in itself, unless one specifies exactly at what intensity is absorption-limited phase matching obtained.

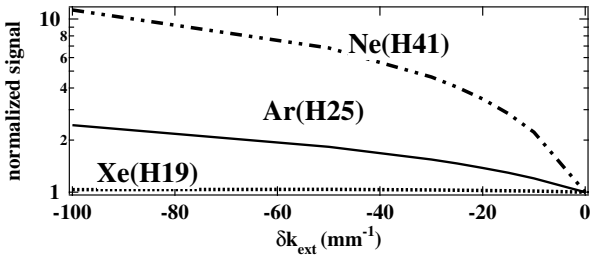

FIG. 4. Yield of harmonics 19 in Xe, 25 in Ar, and 41 in Ne, as a function of an externally imposed wave vector mismatch δk_{ext}, accounting, e.g., for the effect of quasi-phase-matching.

The atomic phase gradient acts as an additional time-dependent wave vector δk_{ext} that allows to compensate for higher electronic dispersions. More generally, we can investigate whether the yields may be increased even further, if one could impose artificially a larger external wave vector. Several new schemes such as quasi-phase-matching [17,18] or self-phase-matching for ultrashort pulses [19] were indeed brought forward to improve phase matching of high harmonics. Our model can be easily generalized by introducing such an external mismatch δk_{ext}, to account for these new phase-matching schemes.

Figure 4 displays the harmonic yield enhancement predicted in absorption-limited conditions as a function of δk_{ext} and for various gases. No improvement appears for Xe, while an enhancement of only 2 is predicted on Ar, equivalent to what we observe experimentally thanks to the dipole phase gradient. In contrast, a large enhancement is obvious in neon. This differing behavior between heavy and light noble gases results from two combined factors. First, the atomic dispersion of Xe and Ar is high, implying little need for additional positive dispersion factors, whereas it is almost zero for light gases. Second, the effective nonlinear coefficient ν is much larger for Ne and He (5.7 for Ne in our conditions, against 3 for Xe), allowing the efficiency to gain strongly even from a modest increase of the intensity at the time of phase matching. These predictions are totally consistent with the experimental quasi-phase-matching results of Paul *et al.* [18].

In conclusion, we could explore directly the phase-matching regime of high harmonics by means of variable-length gas cells, and experimentally evaluate the coherence length of the process. Record conversion efficiencies were demonstrated in argon, in a regime where dipole phases play an important role. These results were explained by investigating how macroscopic yields of high harmonic generation sources may vary, even in absorption-limited conditions. We have emphasized that harmonic generation in freely propagating and guided-wave geometries become equivalent in the long focusing limit, for which an empirical criterion was derived. We have then shown that any description of absorption-limited harmonic emission should make clear the intensity at which phase matching is realized. Large differences between published data can henceforth be explained, in particular, between the low-laser energy guided-wave geometries, and the loosely focused beam ones allowed by high-energy laser systems. Finally, our model shows that the advanced phase-matching schemes currently under development [17–19] should boost the yields for light noble gases only, even in the 10 to 20 nm region for which absorption-limited results were reported. These results should help to reconcile controversial results on absorption-limited conversion efficiencies and stimulate new efforts in this wavelength region of particular technological interest.

[1] P.-M. Paul *et al.*, Science **292**, 1689 (2001).
[2] M. Hentschel *et al.*, Nature (London) **414**, 509 (2001).
[3] A. Rundquist, C. G. Durfee III, Z. Chang, C. Herne, S. Backus, M. M. Murnane, and H. C. Kapteyn, Science **280**, 1412 (1998).
[4] E. Constant *et al.*, Phys. Rev. Lett. **82**, 1668 (1999).
[5] M. Schnürer, Z. Cheng, M. Hentschel, G. Tempea, P. Kálmán, T. Brabec, and F. Krausz, Phys. Rev. Lett. **83**, 722 (1999).
[6] E. Takahashi, Y. Nabekawa, T. Otsuka, M. Obara, and K. Midorikawa, Phys. Rev. A **66**, 021802(R) (2002).
[7] J.-F. Hergott *et al.*, Phys. Rev. A **66**, 021801(R) (2002).
[8] C.-G. Wahlström *et al.*, Phys. Rev. A **48**, 4709 (1993).
[9] P. D. Maker, R.W. Terhune, M. Nisenoff, and C. M. Savage, Phys. Rev. Lett. **8**, 21 (1962).
[10] A. L'Huillier, Ph. Balcou, and L.-A. Lompré, Phys. Rev. Lett. **68**, 166 (1992).
[11] S. Kazamias *et al.*, Eur. Phys. J. D **21**, 353 (2002).
[12] P. Salières, A. L'Huillier, and M. Lewenstein, Phys. Rev. Lett. **74**, 3776 (1995).
[13] Ph. Balcou, P. Salières, A. L'Huillier, and M. Lewenstein, Phys. Rev. A **55**, 3204 (1997).
[14] C. G. Durfee, A. Rundquist, S. Backus, C. Herne, M. M. Murnane, and H. C. Kapteyn, Phys. Rev. Lett. **83**, 2187 (1999).
[15] M. Lewenstein, P. Salières, and A. L'Huillier, Phys. Rev. A **52**, 4747 (1995).
[16] M. B. Gaarde and K. J. Schaffer, Phys. Rev. A **65**, 031406(R) (2002).
[17] S. L. Voronov *et al.*, Phys. Rev. Lett. **87**, 133902 (2001).
[18] A. Paul *et al.*, Nature (London) **421**, 51 (2003).
[19] M. Geissler *et al.*, Phys. Rev. A **62**, 033817 (2000).